

Chapter

2

Synthesis and Characterization
of Unsupported and Supported
Undecamolybdophosphates

Cite this: *Dalton Trans.*, 2011, **40**, 348

www.rsc.org/dalton

PAPER

Novel heterogeneous catalyst, supported undecamolybdophosphate: synthesis, physico-chemical characterization and solvent-free oxidation of styrene

Soyeb Pathan and Anjali Patel*

Received 8th September 2010, Accepted 5th October 2010

DOI: 10.1039/c0dt01187h

A novel heterogeneous catalyst comprising undecamolybdophosphate and hydrous zirconia was synthesized, characterized by various physicochemical techniques and used as an efficient heterogeneous catalyst for oxidation of styrene using H_2O_2 as an oxidant. The novelty of the present work lies in obtaining >99% conversion of styrene with >99% selectivity for benzaldehyde under solvent free mild reaction conditions.

Solvent Free Selective Oxidation of Styrene and Benzyl Alcohol to Benzaldehyde over an Eco-Friendly and Reusable Catalyst, Undecamolybdophosphate Supported onto Neutral Alumina

Anjali Patel* and Soyeb Pathan

Department of Chemistry, Faculty of Science, M. S. University of Baroda, Vadodara 390002, India

 Supporting Information

ABSTRACT: Supported undecamolybdophosphate was synthesized and characterized by various physicochemical techniques and successfully used for solvent free oxidation of styrene and of benzyl alcohol to benzaldehyde. Influence of the reaction parameters (molar ratio of substrate to H_2O_2 , amount of the catalyst, reaction time, and reaction temperature) were studied. The catalyst was reused three times without any significant loss in the catalytic activity. FT-IR, XRD, and DRS of regenerated catalyst indicated that the catalyst was undegraded and stable after the reaction. The novelty of the work lies in obtaining a single selective product, benzaldehyde, as well as a high TON for the same, under mild conditions.

SYNTHESIS

PMo₁₁ was synthesized (as shown in Figure 1) and isolated as sodium salt.

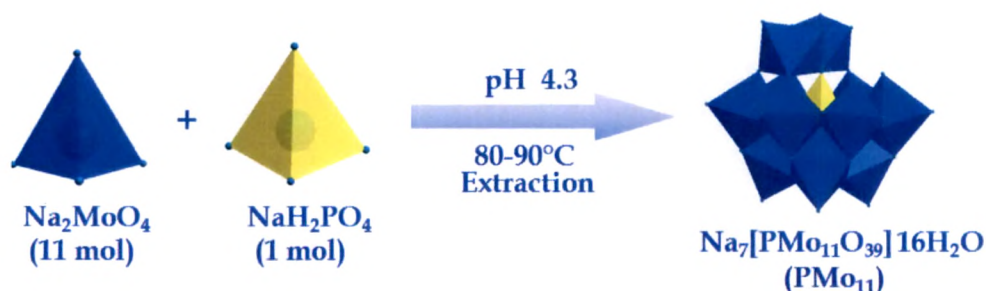


Figure 1. Synthesis of PMo₁₁

Hydrous zirconia and neutral alumina were selected as supports. The main reasons of selecting hydrous zirconia as a support are (i) the available surface hydroxyl groups of hydrous zirconia (ZrO₂) are able to undergo a strong interaction with LPOMs (ii) our expertise in using ZrO₂ as a support [1-21]. It is well known that basic support cannot be used for supporting POMs, since it gets decomposed on the same. So, in the present study we have made use of neutral alumina (Al₂O₃). Al₂O₃ is available in 3 different pH ranges: basic, acidic and neutral. Al₂O₃ at pH of 6-8 is best as a support.

The present chapter describes synthesis and characterization of the unsupported PMo₁₁, and supported PMo₁₁ on two different supports, ZrO₂ and Al₂O₃. Synthesized PMo₁₁ was characterized by various physicochemical techniques such as Elemental analysis (EDS), Thermal analysis (Thermo Gravimetric-Differential Thermal Analysis; TG-DTA), Fourier Transform Infrared Spectroscopy (FT-IR), ³¹P Magic-Angle Spinning Nuclear Magnetic Resonance (³¹P MAS- NMR), Diffused Reflectance Spectra (DRS) and Powder X-ray Diffraction (XRD). Two series of catalysts comprising 10-40% loading of PMo₁₁

onto ZrO_2 and Al_2O_3 were synthesized using incipient impregnation. The supported catalysts were characterized by EDS, Surface Area Measurement (BET method), TG-DTA, FT-IR, ^{31}P MAS NMR, DRS, Powder XRD, and Scanning Electron Microscopy (SEM).

EXPERIMENTAL

Materials

All chemicals used were of A. R. grade. Disodium hydrogen phosphate (Na_2HPO_4), Sodium molybdate dihydrate ($\text{Na}_2\text{MoO}_4 \cdot 2\text{H}_2\text{O}$), Neutral alumina, Acetone and Conc. HNO_3 were obtained from Merck and Zirconium oxychloride ($\text{ZrOCl}_2 \cdot 8\text{H}_2\text{O}$) was obtained from Loba Chemie and used as received.

Synthesis of Na salt of Undecamolybdophosphate (PMo_{11}):

Sodium molybdate dihydrate (0.22 mol, 5.32 g) and anhydrous disodium hydrogen phosphate (0.02 mol, 0.28 g) were dissolved in 50–70 mL of conductivity water and heated to 80–90 °C followed by the addition of concentrated nitric acid in order to adjust the pH to 4.3. The volume was then reduced to half by evaporation and the heteropolyanion was separated by liquid–liquid extraction with 50–60 mL of acetone. The extraction was repeated until the acetone extract showed absence of NO_3^- ions (ferrous sulfate test). The extracted sodium salt was dried in air. The obtained sodium salt of undecamolybdophosphate was designated as PMo_{11} .

Synthesis of the Catalysts

Synthesis of the support, hydrous zirconia (ZrO_2)

Hydrous zirconia was prepared by adding an aqueous ammonia solution to an aqueous solution of $\text{ZrOCl}_2 \cdot 8\text{H}_2\text{O}$ up to pH 8.5. The precipitates were aged at 100°C over a water bath for 1 h, filtered, washed with conductivity water until

chloride free water was obtained and dried at 100°C for 10 h. The obtained material is designated as ZrO₂.

Supporting of PMo₁₁ onto ZrO₂ (PMo₁₁/ZrO₂):

PMo₁₁ was supported on ZrO₂ by dry impregnating method. 1g of ZrO₂ was impregnated with an aqueous solution of PMo₁₁ (0.1g/10 mL of double distilled water). The water from the suspension was allowed to evaporate at 100 °C in an oven. Then the resulting mixture was dried at 100 °C with stirring for 10 h. The material thus obtained was designated as 10% PMo₁₁/ZrO₂. Same procedure was followed for the synthesis of a series of supported PMo₁₁ containing 20-40% PMo₁₁ (0.2 - 0.4g/20 - 40mL of conductivity water). The obtained materials were designated as 20% PMo₁₁/ZrO₂, 30% PMo₁₁/ZrO₂ and 40% PMo₁₁/ZrO₂ respectively.

Supporting of PMo₁₁ onto Al₂O₃ (PMo₁₁/Al₂O₃):

A series of catalysts containing 10–40% PMo₁₁ were synthesized by impregnating 1 g of Al₂O₃ with an aqueous solution of PMo₁₁ (0.1-0.4 g in 10-40mL of conductivity water) with stirring for 35 h and then dried at 100 °C for 10 h. The obtained materials were designated as 10% PMo₁₁/Al₂O₃, 20% PMo₁₁/Al₂O₃, 30% PMo₁₁/Al₂O₃ and 40% PMo₁₁/Al₂O₃.

CHARACTERIZATION

Characterization is a central aspect of catalyst development [22-24]. The elucidation of the structures, compositions, and chemical properties of both the supports used in heterogeneous catalysis as well as the active species present on the surfaces of the supported catalysts is very important for a better understanding of the relationship between catalyst properties and catalytic performance [24].

In case of supported catalysts, it is crucial to know if the active ingredient is on the surface of the support or diffuse in it. As a result from the scientific point of view, the investigation of the surface composition as well as local structure of catalyst at the atomic level and the correlation of these data with catalyst performance is very important in the catalytic reaction. The basic information on the structure-catalytic property relationship for catalyst systems will ultimately be of value in the design of new efficient catalysts [25]. A representative diagram describing the correlation between the active species and the support is shown in Figure 2.

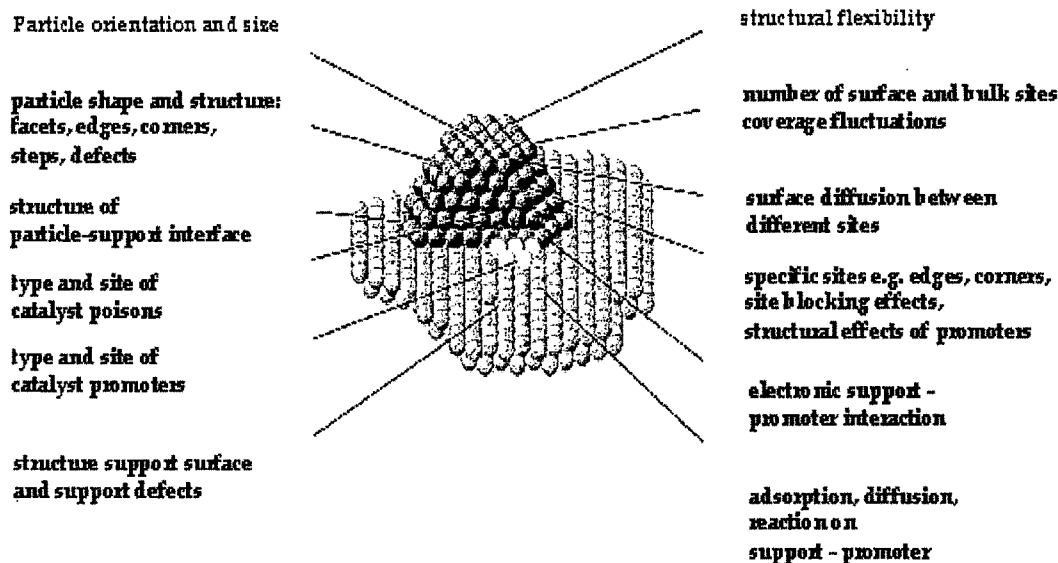


Figure 2. Co-relation of active catalyst species with support

During the last few years many techniques for determining chemical composition, electronic properties and the structure of the upper atomic layers of solids have reached maturity.

Heterogeneous catalyst can be characterized by various tools which comprise different physic-chemical and spectroscopic techniques that are summarized in block diagram shown in Figure 3.

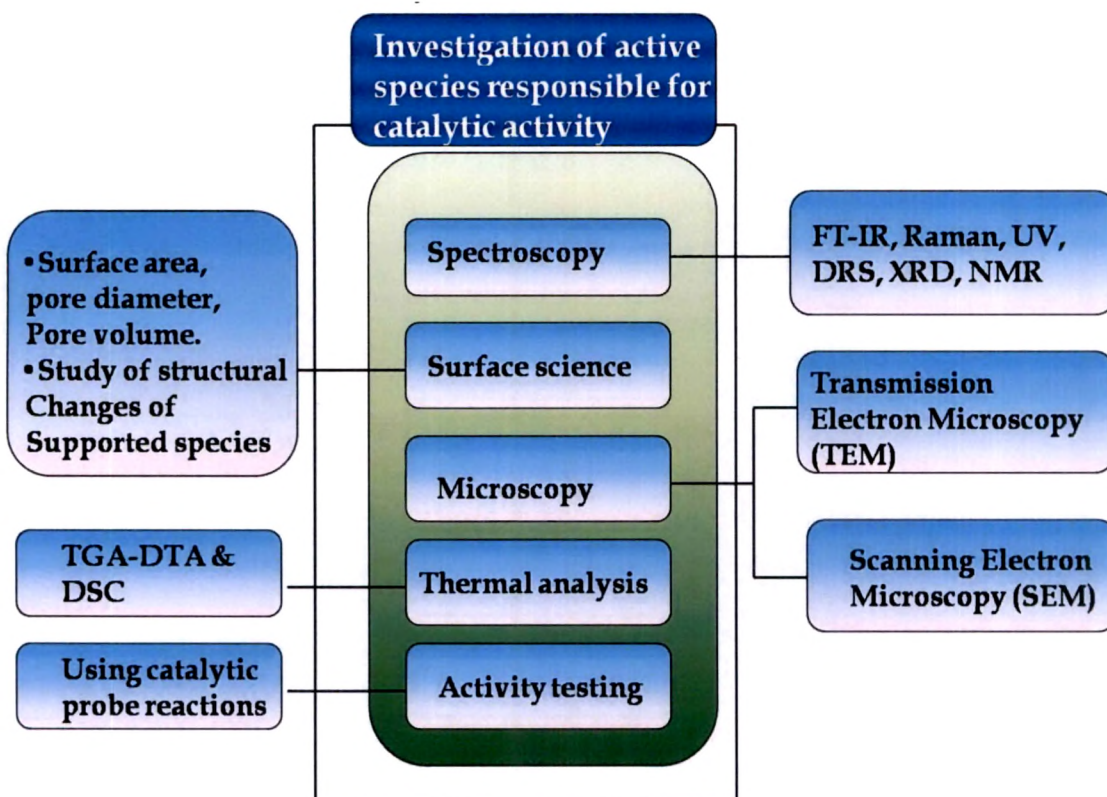


Figure 3. Block diagram of various techniques used in characterization of catalyst

In the present work technique such as EDS, BET Surface Area, TG-DTA, FT-IR, ³¹P MAS NMR, DRS, Powder XRD, and SEM analysis were used for characterization of unsupported and supported PMo₁₁.

Thermal Analysis (Thermo Gravimetric- Differential Thermal Analysis; TG-DTA)

It is a technique whereby the weight of a substance, in an environment heated or cooled at a controlled rate, is recorded as a function of time or temperature. The temperature-weight loss profile of a supported catalyst can provide important quantitative information on the types of water present in the sample. It is usually possible to distinguish loosely held “physisorbed” water from strongly bonded

“chemisorbed” water and helps determine the best conditions for removing the former. More usefully, the study of the decomposition of less stable catalysts can also be done which help in determine the maximum activation temperatures and the temperatures at which the supported reagents can be safely used in reactions. The total weight loss was calculated by the TG-DTA method on the Mettler Toledo Star SW7.01 up to 600 °C.

Fourier Transform Infrared Spectroscopy (FT-IR)

FT-IR spectroscopy is probably the most useful and widely used technique to study supported reagents. It provides following information; Identification of the surface species by identification of functional groups; Dispersion of the reagent over the support surface; Surface activity studies with the use of probe molecules;

FTIR spectra of the samples were recorded as the KBr pellet on the Perkin Elmer instrument.

³¹P Magic-Angle Spinning Nuclear Magnetic Resonance (³¹P MAS- NMR)

The chemical shift and the coupling constants provide information on the static as well as dynamic properties of molecules. The presence and the absence of the functional groups and their quantitative estimation can be made from the chemical shifts. The coupling constants provide information on the molecular structure and conformation.

³¹P MAS NMR spectra were recorded on a Bruker Advance DSX- 300 NMR spectrometer at 121.48 MHz using a 7 mm rotor probe with 85% phosphoric acid as an external standard. The spinning rate was 4–5 kHz.

Diffused Reflectance Spectra (DRS)

The DRS gives information about the non-reduced heteropolyanion due to charge transfer from oxygen to metal. The DRS of sample were recorded at room

temperature on Perkin Elmer 35 LAMDA instrument using barium sulphate as a reference. BaSO₄ was used as a reference. Even though the background was measured independently of the sample the measurements were always performed in double beam mode to compensate for instabilities.

Powder X-ray Diffraction (XRD)

X-ray diffraction is an extremely useful technique in catalysis laboratories, because it allows characterizing the crystal structure of solid materials. From the broadening analysis of the most intense diffraction peaks or from the X-ray distribution at low diffraction angles, the crystal size of a given crystalline phase can be determined.

The powder XRD pattern was obtained by using the instrument Philips Diffractometer (Model PW- 1830). The conditions used were Cu Ka radiation (1.5417Å°).

Surface Area Measurement (Brunauer-Emmett-Teller method; BET surface area)

In case of catalysis, especially, heterogeneous catalysis the reaction follows the surface adsorption phenomenon rather than the typical bulk type catalysis. Hence, the catalytic surfaces need to be characterized by their physical properties. As surface area of the catalyst is directly proportional to the catalytic activity of the heterogeneous catalysts, the measurement of the surface area is most important study for the same.

The BET specific surface area was calculated by using the standard Brunauer, Emmett and Teller method on the basis of the adsorption data. Adsorption-desorption isotherms of samples were recorded on a micromeritics ASAP 2010 surface area analyzer at -196 °C.

Scanning Electron Microscopy (SEM)

SEM provides morphological and topological information about the surfaces of solids that is usually necessary in understanding the behavior of the surfaces. SEM is often the first step in the study of the surface properties of a solid material. The surface of a solid sample is swept in a raster pattern with a finely focused beam of electrons or with a suitable probe. The surface morphology of the support and the supported polyoxoanions were studied.

SEM has been used successfully to study reagent dispersion and surface morphologies. SEM can prove to be more sensitive technique than XRD to study reagent dispersion.

SEM and elemental analysis were carried out using JSM 5610 LV combined with INCA instrument for EDX-SEM.

RESULTS AND DISCUSSION

Characterization of unsupported PMo_{11}

Elemental Analysis

The PMo_{11} was isolated as the sodium salt after completion of the reaction and the remaining solution was filtered off. The filtrate was analyzed to estimate the amount of non reacted Mo [26]. The observed % of Mo in the filtrate was 0.5%, which corresponds to loss of one equivalent of Mo from $\text{H}_3\text{PMo}_{12}\text{O}_{40}$. The observed values for the elemental analysis are in good agreement with the theoretical values indicating the formation of PMo_{11} . Anal. calc. (%): Na, 7.65; Mo, 50.12; P, 1.47; O, 39.52. Found (%): Na, 7.60; Mo, 49.99; P, 1.44; O, 39.92.

TG-DTA

The TG-DTA curve of PMo_{11} is presented in Figure 4. The TGA of PMo_{11} shows an initial weight loss of 16% from 30–150 °C. This may be due to the removal of adsorbed water and water of crystallization. The final weight loss at around 235°C indicates the decomposition of PMo_{11} .

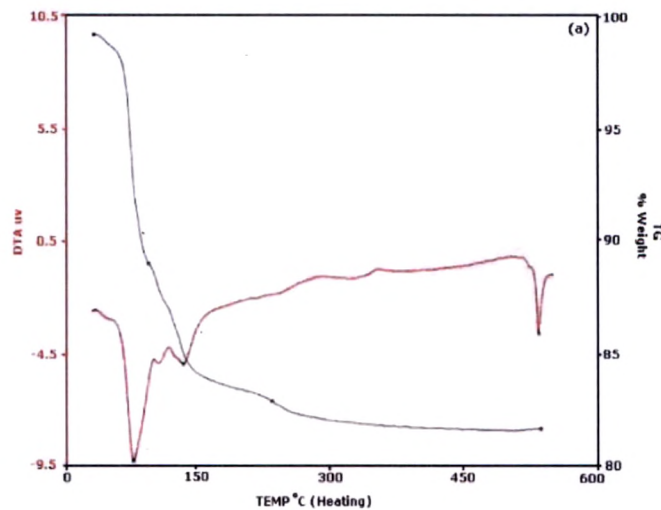


Figure 4. TG-DTA of PMo_{11}

DTA of PMo_{11} (Figure 4) shows endothermic peaks at 80 °C and 140 °C, due to the loss of adsorbed water and water of crystallization respectively. In addition, DTA of PMo_{11} also shows a broad exothermic peak in the region of 270–305 °C. This may be due to the decomposition of PMo_{11} .

Number of water molecules was determined from the TGA curve using the following formula

$$18n = \frac{X(M + 18n)}{100}$$

Where, n = number of water molecules

X = % loss from TGA

M = molecular weight (without water of crystallization)

Based on studies the chemical formula of the isolated sodium salt was proposed as



FT-IR

The FT-IR spectra of PMo_{12} and PMo_{11} are presented in Figure 5. The bands at 1070 cm^{-1} , 965 cm^{-1} , 870 cm^{-1} , 790 cm^{-1} in parent Keggin PMo_{12} attributed to asymmetric stretches of P-O_a , Mo-O_t , Mo-O-Mo .

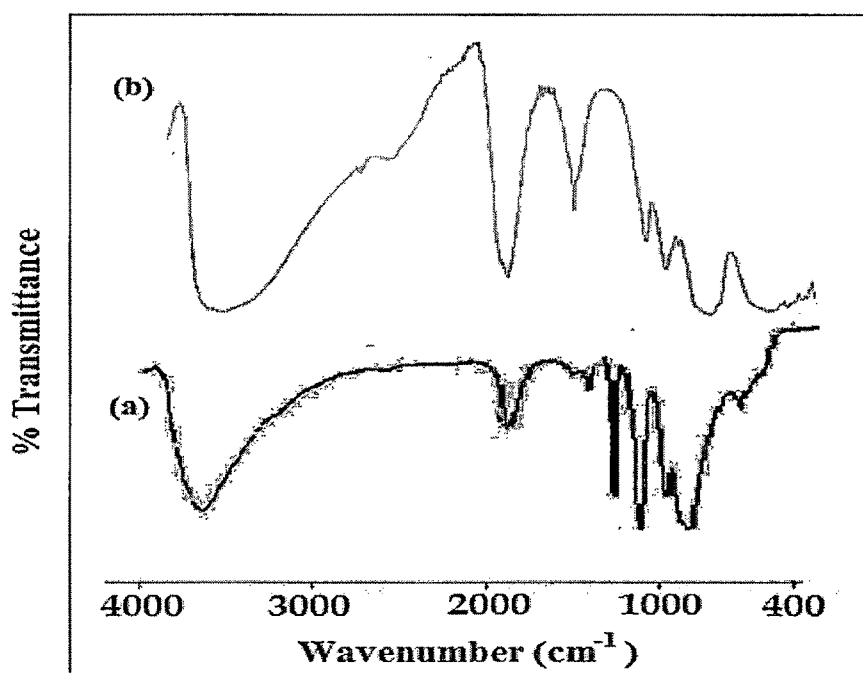


Figure 5. FT-IR spectra for (a) PMo_{12} and (b) PMo_{11}

The FT-IR spectra of PMo_{11} shows P-O_a band at 1048 and 999 cm^{-1} . Observed splitting for P-O_a band in PMo_{11} as compare to that of PMo_{12} , indicates formation of lacunary structure with Keggin unit. The FT-IR spectra of PMo_{11} also shows bands 935 and 906 cm^{-1} and 855 cm^{-1} attributed to asymmetric stretches of Mo-O_t



and Mo-O-Mo, respectively and are in good agreement with reported values [27]. The shifting in the band position may be due to formation of lacuna in synthesized material.

³¹P NMR

The ³¹P chemical shift provides important information concerning the structure, composition and electronic states of these materials. ³¹P MAS NMR of PMO₁₁ is presented in Figure 6.

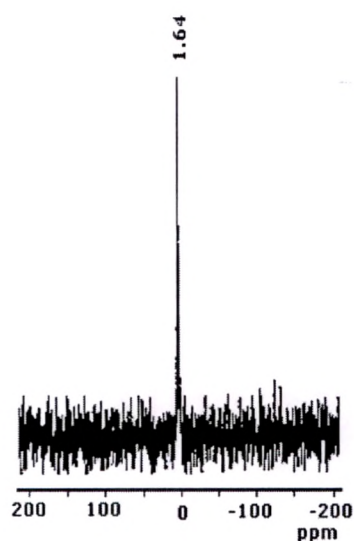


Figure 6. ³¹P MAS NMR of PMO₁₁

As discussed earlier, Van-Veen reported in acidic solution, phosphomolybdate was present in different type of species (e.g. [P₂Mo₅O₂₃]⁶⁻, [PMo₆O₂₅]⁹⁻, [PMo₉O₃₁.(OH)₃]⁶⁻, [PMo₁₀O₃₄]³⁻, [PMo₁₁O₃₉]⁷⁻ and [PMo₁₂O₄₀]³⁻) in the acidified aqueous solution [28]. The ³¹P MAS NMR spectra shows single peak at 1.64 ppm corresponds to PMO₁₁ which also indicates absence of fragmentation of PMO₁₁.

DRS

DRS of PMo_{12} and PMo_{11} are presented in Figure 7. DRS of PMo_{12} shows band at 280 nm (λ_{max}) attributed to O \rightarrow Mo charge transfer in Keggin unit. Similar, charge transfer is observed for PMo_{11} at 290 nm. In other words, PMo_{11} retains its Keggin structure.

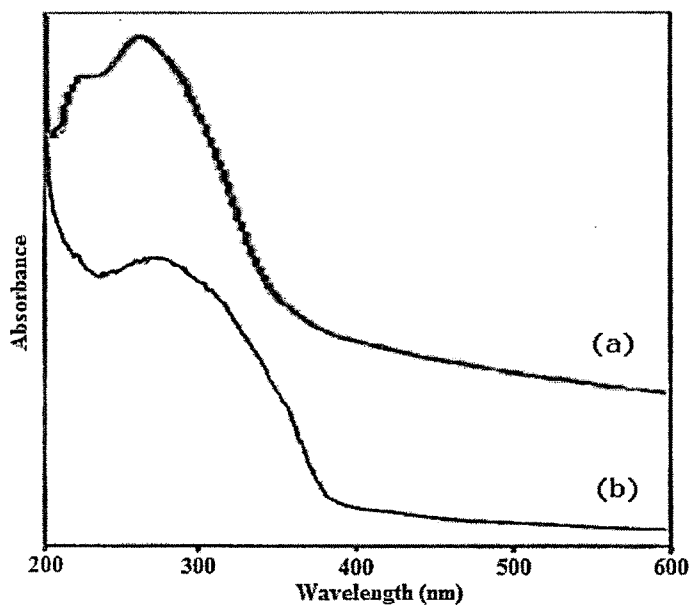


Figure 7. DRS of (a) PMo_{12} and (b) PMo_{11}

Powder XRD

The powder X-ray pattern for PMo_{12} and PMo_{11} is represented in Figure 8.

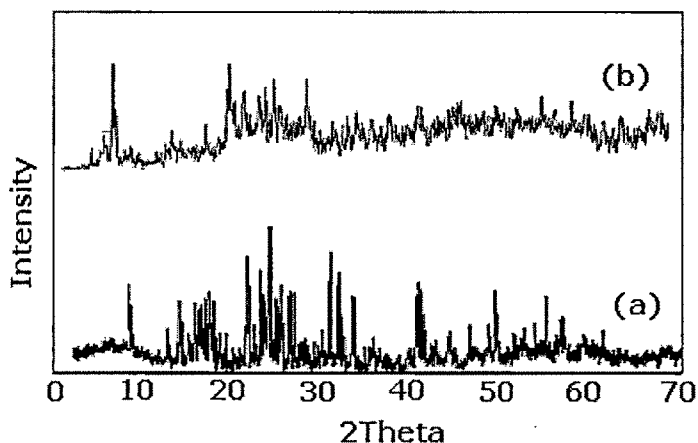


Figure 8. Powder XRD pattern of (a) PMo_{12} and (b) PMo_{11}

The powder XRD pattern of the isolated sodium salt indicates the semi-crystalline nature of PMo_{11} . PMo_{11} shows the characteristic diffraction patterns with the typical 2θ value of $8-10^\circ$ indicating the formation of lacunary molybdophosphate specie. For PMo_{11} , similar peaks with shifting as compare to that of PMo_{12} were observed indicates presence of Keggin unit.

Thus the thermal, spectral as well as diffraction studies confirms the formation of PMo_{11} .

Characterization of supported PMo_{11}

Chemical Stability

Chemical stability of a catalyst plays an important role. The materials which have a high solubility in water and/or in acidic media may not be very useful. It is advisable to have a rough guide of the solubility of the material being used as a catalyst. The stability of all the synthesized materials have to be check in different acids and bases.

The supported catalysts were evaluated for chemical stability and the present catalysts, shows no change in color or form on heating with water. The materials are stable in different mineral acids like HCl , H_2SO_4 , HNO_3 and bases like NaOH , Na_2O_3 etc. up to $\sim 2\text{M}$ concentration.

Leaching Test

Leaching is a negative property for any catalyst. Any leaching of the catalyst from the support would make the catalyst unattractive for reusing. So, it is necessary to study the stability of polyanion onto support in order to reuse the catalyst. When the polyoxometalate react with a mild reducing agent such as ascorbic acid [29], it develops blue colouration, which can be used for the quantitative characterization for the leaching of polyoxometalate from the support. In the current work, we have used this method for determining the leaching of PMo_{11} from zirconia and neutral alumina.

Standard samples amounting to 1-5% of PMo_{11} in water were prepared. To 10mL of the above samples, 1mL of 10% ascorbic acid was added. The mixture was diluted to 25mL. The resultant solution was scanned at a λ_{max} of 785 cm^{-1} for its

absorbance values. A standard calibration curve was obtained by plotting values of absorbance with percentage solution. One gram of 20%-PMo₁₁/ZrO₂ as well as 20%-PMo₁₁/Al₂O₃ was refluxed for 4h with 10mL of conductivity water. 1mL of the supernant solution was then treated with 10% ascorbic acid. No development of blue color indicates no leaching. The same procedure was repeated with water, styrenes, cyclohexene, cyclooctene, benzyl alcohol, cyclopentanol, cyclohexanol, 1-hexanol, 1- octanol and also with the filtrates of all the reaction mixtures after completion of the reaction. The above procedure was followed for all catalysts and no leaching was found. For each case, absence of blue color indicates no leaching of PMo₁₁ from support into reaction medium. The study indicates the presence of chemical interaction between the PMo₁₁ and the supports, as well as stability of the resultant catalysts under reaction conditions.

BET

The values of surface area for both the series of catalysts are shown in Table 1 and Table 2.

Table 1 Surface Area of PMo₁₁/ZrO₂ series

Catalysts	Surface area (m ² /g)
ZrO ₂	170
10% PMo ₁₁ /ZrO ₂	191
20% PMo ₁₁ /ZrO ₂	197
30% PMo ₁₁ /ZrO ₂	188
40% PMo ₁₁ /ZrO ₂	187

Table 2 Surface Area of $\text{PMo}_{11}/\text{Al}_2\text{O}_3$ series

Catalysts	Surface area (m^2/g)
Al_2O_3	81.0
10% $\text{PMo}_{11}/\text{Al}_2\text{O}_3$	99.7
20% $\text{PMo}_{11}/\text{Al}_2\text{O}_3$	101.8
30% $\text{PMo}_{11}/\text{Al}_2\text{O}_3$	72.9
40% $\text{PMo}_{11}/\text{Al}_2\text{O}_3$	56.2

It is seen from Tables that, initially the value for surface area increases with increase in loading from 10% to 20% while it decreases from 20% to 40%. This may be due to the formation of multilayers of active species, PMo_{11} , onto support surface, which may cause blocking/stabilization of active sites on the monolayer.

From Table 1 and 2, it is clear that highest surface area was observed for 20% $\text{PMo}_{11}/\text{ZrO}_2$ and 20% $\text{PMo}_{11}/\text{Al}_2\text{O}_3$. Hence, 20 % loaded catalysts were selected for detail characterizations.

TG-DTA

The TGA of 20% $\text{PMo}_{11}/\text{ZrO}_2$ (Figure 9) shows initial weight loss up to 150 °C may be due to the removal of adsorbed water molecules. No significant loss occurs *after* 300 °C, which indicates increase in the stability of PMo_{11} after supporting on ZrO_2 .

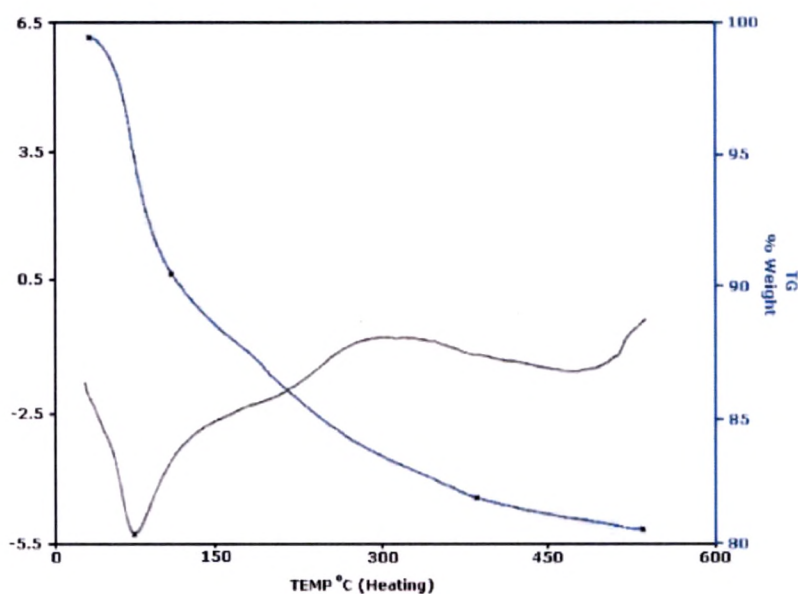


Figure 9. TG-DTA of 20% $\text{PMo}_{11}/\text{ZrO}_2$

DTA of 20% $\text{PMo}_{11}/\text{ZrO}_2$ (Figure 9) shows an endothermic peak at 80 °C which may be due to adsorbed water. It also shows a broad exothermic peak in the region 285–325 °C, which may be due to decomposition of PMo_{11} on to the surface of the support.

The TGA of 20% $\text{PMo}_{11}/\text{Al}_2\text{O}_3$ (Figure 10) shows initial weight loss up to 123 °C and then continues weight loss was observed in the region 250-375 °C may be due to the removal of adsorbed water molecules and crystallization water molecules, respectively.

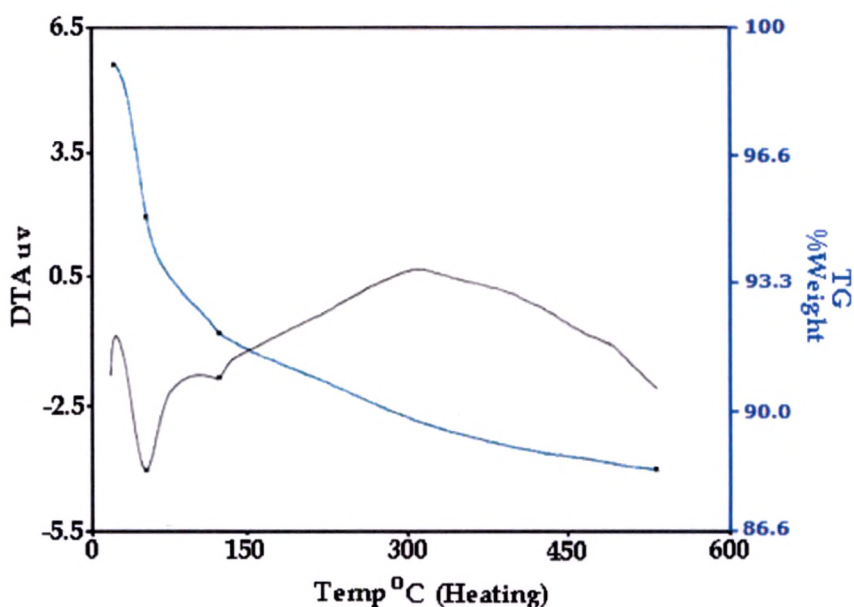


Figure 10. TG-DTA of 20% $\text{PMo}_{11}/\text{Al}_2\text{O}_3$

This observation was further supported by DTA of 20% $\text{PMo}_{11}/\text{Al}_2\text{O}_3$ (Figure 10), which shows endothermic peaks at 80 °C, 140 °C corresponds to removal of adsorbed water molecules and crystallization water, followed by a broad exothermic peak in the region 255-425 °C corresponds to decomposition of PMo_{11} on to the surface of the support.

From the above study it is clearly seen that supporting of PMo_{11} onto different supports, results in increase in the thermal stability of PMo_{11} . Further, it was observed that supported catalysts are stable upto 320 °C.

FT-IR

The FT-IR spectra for ZrO_2 and 20% $\text{PMo}_{11}/\text{ZrO}_2$ are shown in Figure 11. The FT-IR of ZrO_2 shows a broad band in the region of 3400 cm^{-1} . This is attributed to ν_{as} hydroxo (-OH) and aquo (-OH) stretching. Two types of bending vibrations are observed at 1600 and 1370 cm^{-1} indicating the presence of (H-O-H) bending and (O-H-O) bending respectively. It also shows a weak band at 600 cm^{-1} attributed to the presence of Zr-O-H bond.

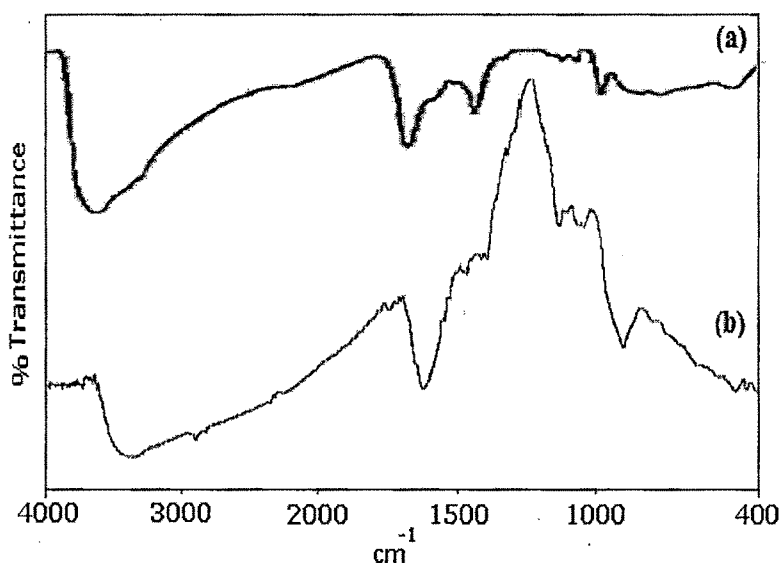


Figure 11. FT-IR spectra of (a) ZrO_2 and (b) 20% $\text{PMo}_{11}/\text{ZrO}_2$

The FT-IR spectra of 20% $\text{PMo}_{11}/\text{ZrO}_2$ (Figure 11) shows a band at 557 cm^{-1} assigned to Zr-O-H stretching. Bands at 1039 cm^{-1} , 990 cm^{-1} and 910 cm^{-1} correspond to asymmetric stretching of P-O_a and Mo-O-Mo, respectively. The shifting of bands as well as the disappearance of the Mo-O_t band (935 cm^{-1}) may be due to interaction of terminal oxygen of PMo_{11} with surface hydrogen of ZrO_2 .

20% $\text{PMo}_{11}/\text{Al}_2\text{O}_3$ (Figure 12) shows vibration bands at 1052 cm^{-1} , 1010 cm^{-1} and 914 cm^{-1} (broad) correspond to asymmetric stretching of P-O_a and Mo-O-Mo , respectively. A broad band of Al_2O_3 covers the small Mo-O_t band (935 cm^{-1}) in 20% $\text{PMo}_{11}/\text{Al}_2\text{O}_3$.

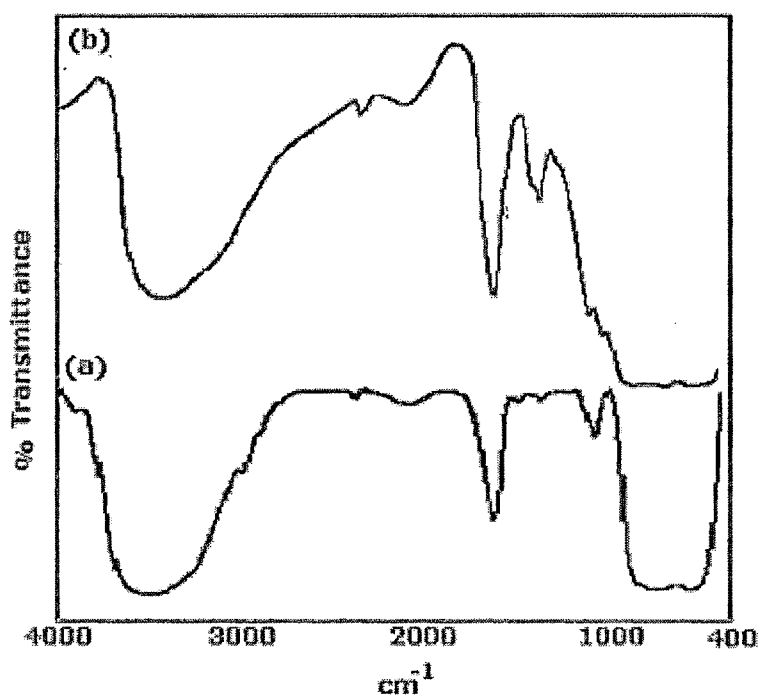


Figure 12. FT-IR spectra of (a) Al_2O_3 and (b) 20% $\text{PMo}_{11}/\text{Al}_2\text{O}_3$

The shifting and broadening of bands may be due to interaction of terminal oxygen of PMo_{11} with Al_2O_3 . The low intensity of the bands may be due to the overlapping of the vibrational frequencies of 20% $\text{PMo}_{11}/\text{Al}_2\text{O}_3$ and Al_2O_3 .

^{31}P MAS NMR

^{31}P MAS NMR spectra of PMo_{11} (Figure 6) show a single peak at 1.64 ppm. While, ^{31}P MAS NMR for 20% $\text{PMo}_{11}/\text{ZrO}_2$ and 20% $\text{PMo}_{11}/\text{Al}_2\text{O}_3$ (Figure 13) reveals resonance at -2.42 ppm and -3.47 ppm respectively.

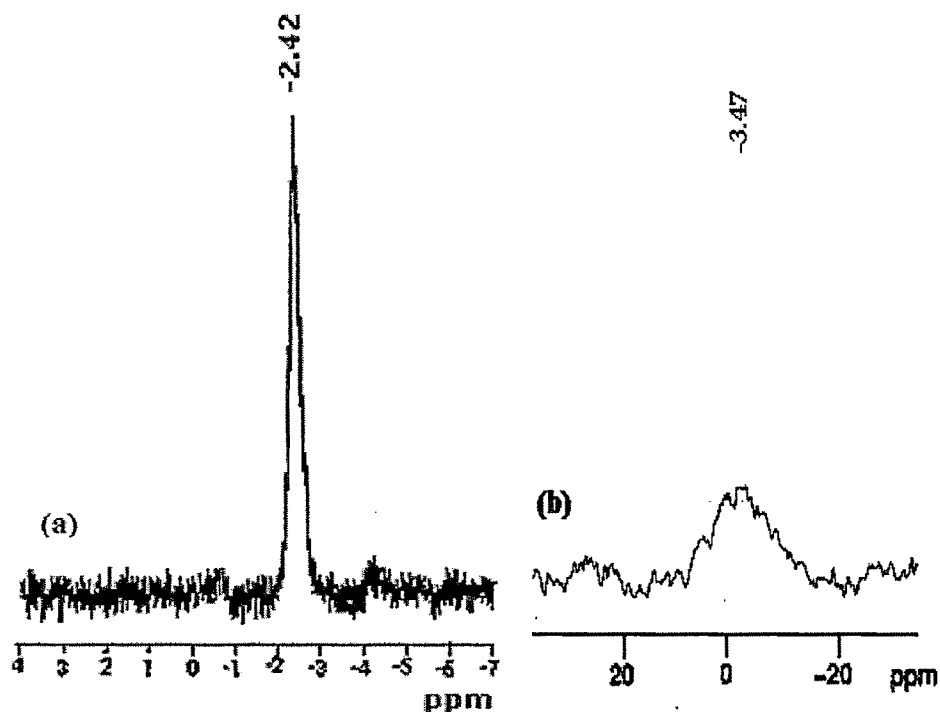


Figure 13. ^{31}P MAS NMR of (a) 20% $\text{PMo}_{11}/\text{ZrO}_2$ and (b) 20% $\text{PMo}_{11}/\text{Al}_2\text{O}_3$

It is reported that the lower shift, i.e. deshielding, increases as the degree of adsorption and degree of fragmentation increases [30]. In the present cases, the observed chemical shift, shielding as compare to that of PMo_{11} , indicates presence of chemical interaction between PMo_{11} and supports, rather than simple adsorption. Also, a single peak for both the catalysts indicated that no fragmentation of PMo_{11} species takes place after addition to the support. Thus it can be concluded that PMo_{11} remains intact on surface of supports, after supporting on to supports.

The difference in nature of the signal as well as values of the NMR shift for 20% $\text{PMo}_{11}/\text{ZrO}_2$ and 20% $\text{PMo}_{11}/\text{Al}_2\text{O}_3$ may be due to the different nature of the supports. It is known that ZrO_2 is an acidic support and it has more surface hydroxyl groups as compare to that of Al_2O_3 for strong interaction through hydrogen bonding with the terminal oxygens of PMo_{11} . Thus, more shielding is observed for Al_2O_3 . Thus the obtained results are in good agreement with the proposed explanation.

DRS

DRS of $\text{PMo}_{11}/\text{ZrO}_2$ shows band at 290 (λ_{max}), attributed to $\text{O} \rightarrow \text{Mo}$ charge transfer. The λ_{max} of 20% $\text{PMo}_{11}/\text{ZrO}_2$ is same as that for PMo_{11} (Figure 14).

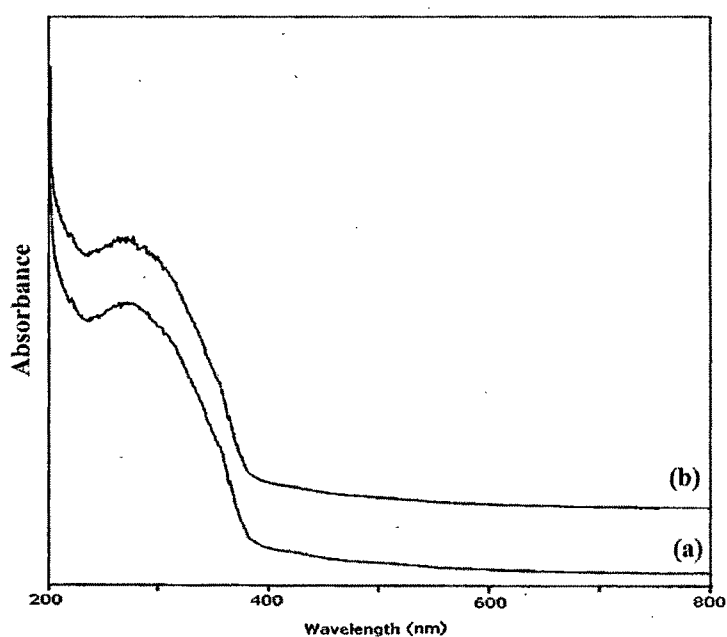


Figure 14. DRS of (a) PMo_{11} and (b) 20% $\text{PMo}_{11}/\text{ZrO}_2$

Similarly, The band at 300 (λ_{\max}) for 20% $\text{PMo}_{11}/\text{Al}_2\text{O}_3$ (Figure 15) is attributed to $\text{O} \rightarrow \text{Mo}$ charge transfer. This confirms the presence of the undegraded PMo_{11} on the surface of ZrO_2 . In other words, the Keggin structure remains unaltered.

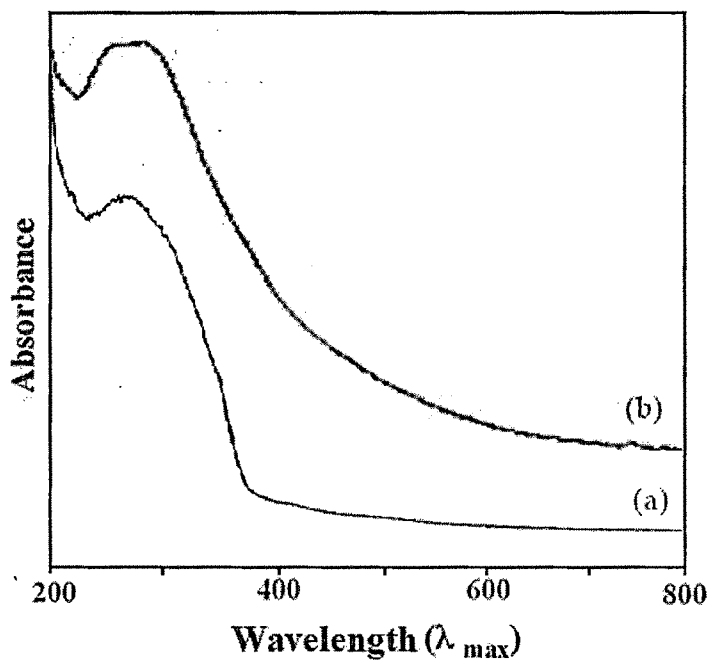


Figure 15. DRS of (a) PMo_{11} and (b) 20% $\text{PMo}_{11}/\text{Al}_2\text{O}_3$

Powder XRD

The XRD pattern of 20% $\text{PMo}_{11}/\text{ZrO}_2$ (Figure 16a) and 20% $\text{PMo}_{11}/\text{Al}_2\text{O}_3$ (Figure 16b) shows the amorphous nature of the materials indicating that the crystallinity of the PMo_{11} is lost after supporting.

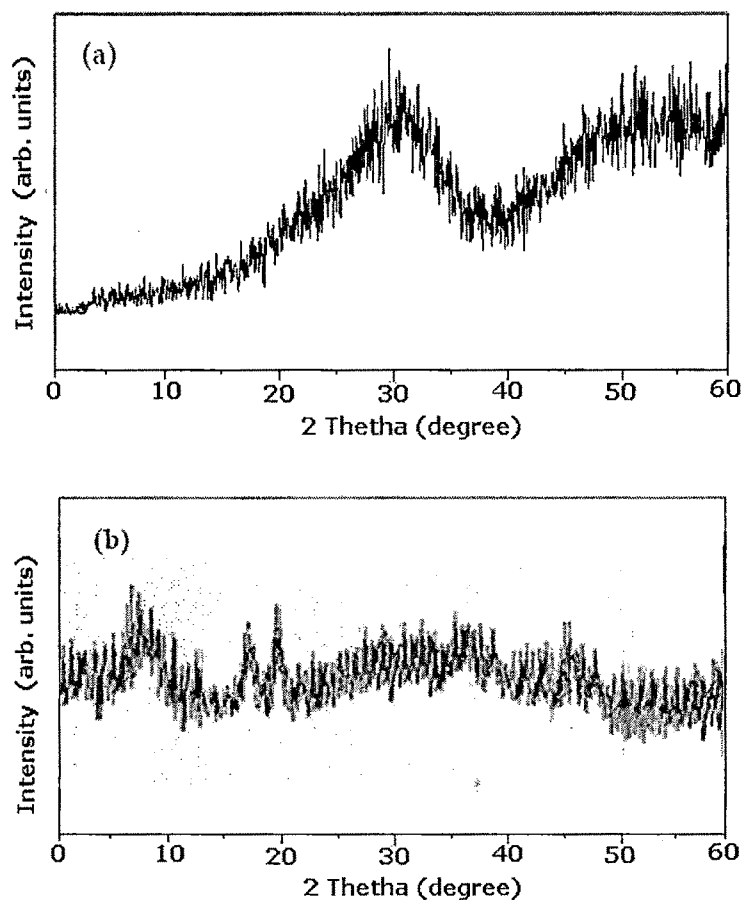


Figure 16. Powder XRD pattern of (a) 20% $\text{PMo}_{11}/\text{ZrO}_2$ and (b) 20% $\text{PMo}_{11}/\text{Al}_2\text{O}_3$

Further, it does not show any diffraction lines of lacunary PMo_{11} indicating a very high dispersion of solute as a non-crystalline form on the surface of the supports.

Scanning Electron Microscopy (SEM)

The catalysts were further characterized for surface morphology. The support and supported PMo_{11} was characterized for the scanning electron microscopy. The scanning electron microscopy (SEM) images of ZrO_2 , PMo_{11} and 20% $\text{PMo}_{11}/\text{ZrO}_2$ at a magnification of 100x are reported in Figure 17.

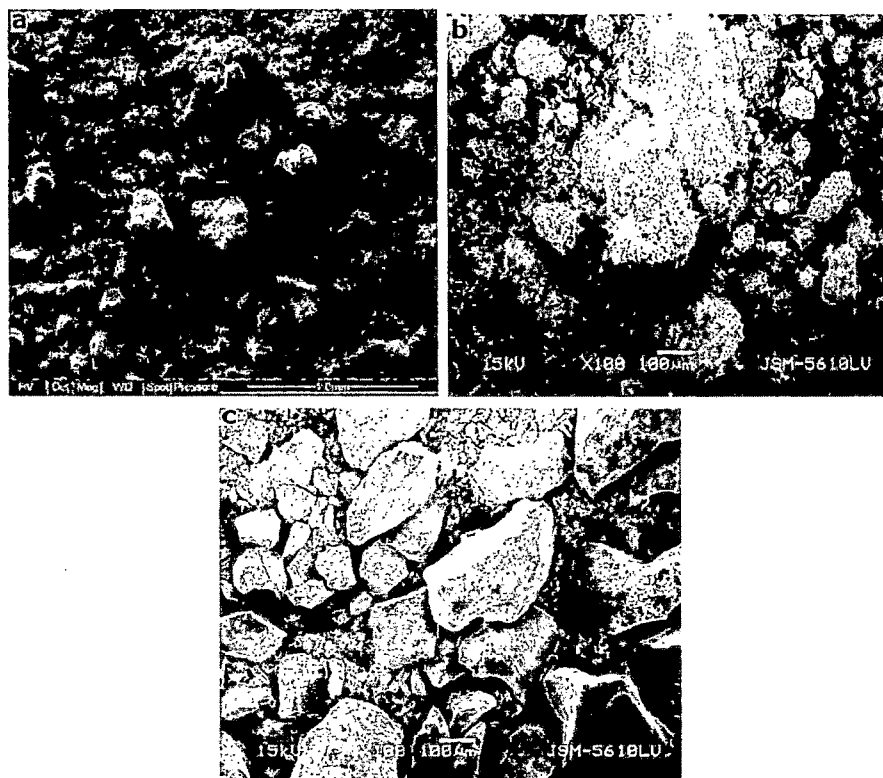


Figure 17. SEM images of (a) ZrO_2 , (b) PMo_{11} and (c) 20% $\text{PMo}_{11}/\text{ZrO}_2$

Figure 17b shows the semi-crystalline nature of PMo_{11} . SEM of 20% $\text{PMo}_{11}/\text{ZrO}_2$ (Figure 17c) shows a uniform dispersion of PMo_{11} in a non-crystalline form on the surface of the support.

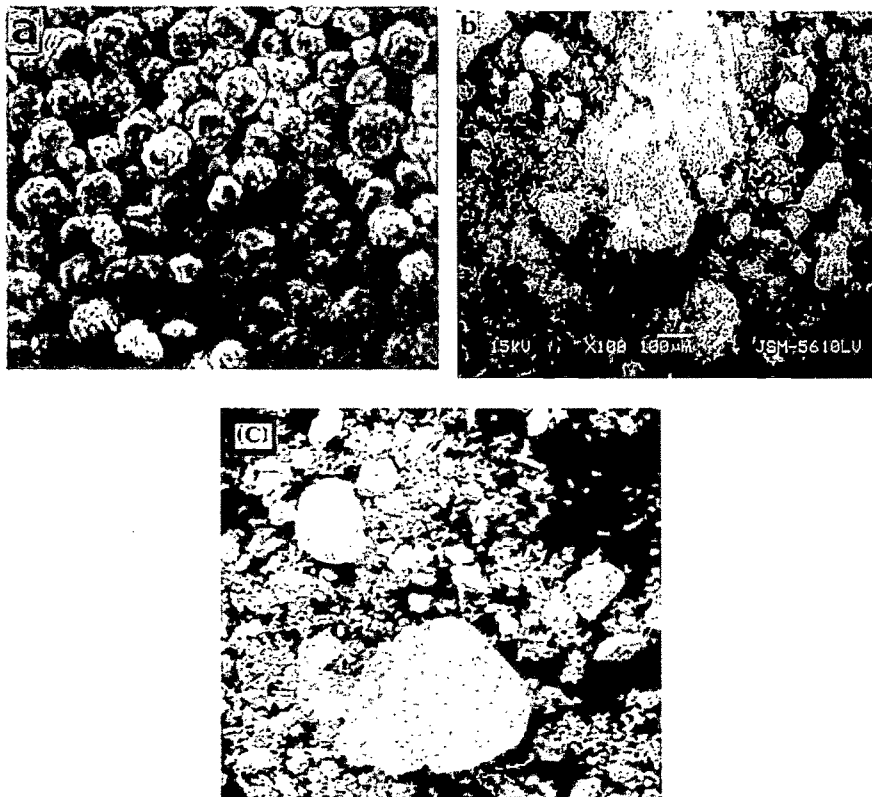
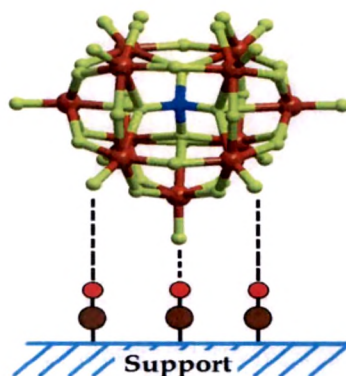


Figure 18. SEM images of (a) Al_2O_3 , (b) PMo_{11} and (c) 20% $\text{PMo}_{11}/\text{Al}_2\text{O}_3$

The SEM images of Al_2O_3 , PMo_{11} and 20% $\text{PMo}_{11}/\text{Al}_2\text{O}_3$ are shown in Figure 18. In order to compare the surface morphology of both the supported catalysts, the SEM pictures were taken at same magnification. It is seen from the figure that surface of the support is distinctly altered. It exhibit considerable surface shinning after supporting of the PMo_{11} . SEM of 20% $\text{PMo}_{11}/\text{Al}_2\text{O}_3$ shows a uniform dispersion of PMo_{11} in a noncrystalline form on the surface of the support.

CONCLUSIONS

1. Synthesis, isolation and stabilization of PMo_{11} was achieved successfully, and confirmed by elemental and spectral studies.
2. Thermal analysis shows that the PMo_{11} does not get disturbed up to 320°C when supported on ZrO_2 and Al_2O_3 .
3. FT-IR, NMR and DRS studies confirm that PMo_{11} retains its Keggin type structure when supported onto ZrO_2 and Al_2O_3 .
4. XRD and SEM studies show the uniform dispersion of PMo_{11} onto the surface of both the supports.
5. ^{31}P MAS NMR indicates the presence of strong interaction between the active species (PMo_{11}) and the supports (ZrO_2 and Al_2O_3)
6. From spectroscopic and surface characterization, the possible interaction between the support and the PMo_{11} is as follows



7. Series of stable catalysts, comprising of PMo_{11} and different supports; $\text{PMo}_{11}/\text{ZrO}_2$ and $\text{PMo}_{11}/\text{Al}_2\text{O}_3$ were synthesized successfully.

REFERENCES

1. Y. Girase, A. Patel, *J. Ind. Chem. Soc.*, 79, 892, (2002).
2. S. Patel, A. Patel, *Ind. J. Chem. Sect A*, 41, (2002).
3. S. Patel, N. Purohit, A. Patel, *J. Mol. Catal. A: Chem.*, 192, 195, (2003).
4. P. Sharma, S. Vyas, A. Patel, *J. Mol. Catal. A: Chem.*, 214, 281, (2004).
5. N. Bhatt, A. Patel, *J. Mol. Catal. A: Chem.*, 238, 223, (2005).
6. P. Sharma, A. Patel, *Bull. Mater. Sci.*, 29, 439, (2006).
7. N. Bhatt, A. Patel, *J. Mol. Catal. A: Chem.*, 275, 14, (2007).
8. N. Bhatt, C. Shah, A. Patel, *Cat. Lett.*, 117, 146, (2007).
9. N. Bhatt, A. Patel, *Cat. Lett.*, 113, 99, (2007).
10. N. Bhatt, A. Patel; *Ind. J. Chem. Sec. A*, 47A, 387, (2008).
11. N. Bhatt, P. Sharma, A. Patel, P. Selvam, *Cat. Commun.*, 9, 1545, (2008).
12. N. Bhatt, A. Patel, *Reac. Kin. Cat. Lett.*, 95, 281, (2008).
13. P. Shringarpure, A. Patel, *Dalton Trans.*, 3953, (2008).
14. P. Sharma, A. Patel, *J. Mol. Catal. A Chem.*, 299, 37, (2009).
15. P. Sharma, A. Patel, *Appl. Surf. Sci.*, 255, 7635, (2009).
16. P. Sharma, A. Patel, *Ind. J. Chem. Sec A*, 48A, 964, (2009).
17. N. Bhatt, A. Patel, *Kin. Cat.*, 50, 401, (2009).
18. P. Shringarpure, A. Patel, *Dalton Trans.*, 39, 2615, (2010).
19. P. Shringarpure, A. Patel, *J. Mol. Catal. A Chem.*, 321, 22, (2010).
20. P. Shringarpure, A. Patel, *Reac. Kinet. Mech. Catal.* 103,165, (2011).
21. N. Bhatt, A. Patel, *J. Taiwan Inst. Chem. Eng.*, 42, 356, (2011).
22. J. M. Thomas, W. J. Thomas, *Principles and Practice of Heterogeneous Catalysis*, VCH, Weinheim, (1997).
23. R. A. van Santen, P. W. N. M. Van Leeuwen, J. A. Moulijn, B. A. Averil (Eds.), *Catalysis: An Integrated Approach*, (2nd ed.), Elsevier, Amsterdam, (1999).

24. R. Richards (ed.), "Surface and Nanomolecular Catalysis", CRC press, Ch 1, p2, (2006).
25. "Spectroscopic Characterization of Heterogeneous Catalysts", J. L. G. Fierro, *Stud. Surf. Sci. Cat.*, Elsevier, vol 57A, (1990).
26. A. Vogel. *A Textbook of Quantitative Inorganic Analysis*, 2nd Edn, Longmans, Green and Co., London (1951).
27. T. Okuhara, N. Mizuno, M. Misono, *Adv. Catal.*, 41, 130, (1996).
28. J. A. R. Van, veen, O. Sundmeijer, C. A. Emeis and H. J. De Wit, *J. Chem. Soc., Dalton Trans.*, 1825, (1986).
29. G. D. Yadav, V. V. Bokade, *Appl. Catal. A Gen.*, 147, 299, (1996).
30. J. C. Edwards, C. Y. Thiel, B. Benac, J. F. Knifton, *Catal. Lett.*, 51, 77, (1998).